

# Geochemical stratigraphy and magmatic evolution at Arenal Volcano, Costa Rica

Louise L. Bolge<sup>a,b,\*</sup>, Michael J. Carr<sup>b</sup>, Mark D. Feigenson<sup>b</sup>, Guillermo E. Alvarado<sup>c</sup>

<sup>a</sup> Boston University, Department of Earth Sciences, 685 Commonwealth Ave, Boston, MA 02215, USA

<sup>b</sup> Rutgers University, Department of Geological Sciences, 610 Taylor Rd, Piscataway, NJ 08854, USA

<sup>c</sup> Observatorio Sismológico y Vulcanológico de Arenal y Miravalles (OSIVAM), Instituto Costarricense de Electricidad (ICE), Apdo. 10032-1000, Costa Rica

Received 13 June 2005; accepted 28 March 2006

Available online 5 July 2006

## Abstract

Arenal has been active for at least the past 7000 years. Prior to 3000 years B.P. (before present), Arenal eruptive products consisted of lavas and tephra both with a mafic (basaltic andesitic) composition. At approximately 3000 years B.P. Arenal began producing two discrete tephra compositions, a mafic (basaltic) tephra and a silicic (andesitic to dacitic) tephra as well as the basaltic andesitic lavas whose composition falls into the gap between the two tephra compositions. The amount of phenocrysts in both the mafic tephra and, to a lesser extent, the lavas, has increased steadily over time, demonstrating a gradual increase in the amount of crystal–liquid fractionation. At approximately 3000 years B.P. the fractionation reached a threshold causing the production of silicic tephra in conjunction with the mafic tephra. Modal analyses show that while the mafic tephra become more crystalline over time, the silicic tephra have become glassier. These younger mafic tephra are mineral-rich residues, while the silicic tephra are the incompatible element rich melt. There is also an increase in the crystal–liquid fractionation within the magma forming the lavas and tephra. The concentration of incompatible elements in the lavas has increased over time, while it has decreased in the tephra. In addition to the crystal–liquid redistribution in the magmas at Arenal, there have also been changes in Arenal's source region. The amount of flux from the subducting slab and consequently the degree of melting increase up to approximately 3000 years B.P., and then begin decreasing.

© 2006 Elsevier B.V. All rights reserved.

*Keywords:* Arenal; magmatic evolution; tephrostratigraphy; Central American arc

## 1. Introduction

Arenal is a small strato volcano located in Costa Rica (10°27.8'N, 84°42.3'W) along the Central American volcanic arc (Malavassi, 1979). On July 29, 1968 Arenal erupted violently with a directed blast (Melson and

Saenz, 1973). Prior to this eruption Arenal was not considered an active volcano. A period of steady-state volcanism followed the directed blast that initiated the current activity (e.g., Alvarado et al., 2006-this volume).

The impressive lava field developing at Arenal has led to thorough investigations of its magmatic evolution (Malavassi, 1979; Kussmaul et al., 1982; Melson, 1982; Tournon, 1984; Cigolini and Bogliotti, 1984, Cigolini and Kudo, 1987, Cigolini, 1998). The geochemistry of the ongoing lava eruption at Arenal (A1) has been documented by

\* Corresponding author. Boston University, Department of Earth Sciences, 685 Commonwealth Ave, Boston, MA 02215, USA.

E-mail address: [bolge@bu.edu](mailto:bolge@bu.edu) (L.L. Bolge).





4000 years to Arenal's history. The stratigraphy and age of each tephra unit are listed in Table 1.

The younger tephtras (ET2 to ET9) have dark carbon-rich paleosols overlying them whereas the older less voluminous tephtra layers do not. Soto et al. (1998) interpreted the change in soil character as the result of a change in climate at Arenal, from a dry environment to a rainy tropical one. The tephtra stratigraphy of Arenal and radiocarbon ages are discussed in detail by Soto and Alvarado (2006-this volume).

### 1.2. Lava stratigraphy

Beneath Arenal's current lava flow field (A1) there are at least four prehistoric lava flow fields: from youngest to oldest: A2, A3, A4, and LA (Borgia et al., 1988). Units A2, A3 and A4 have distinctive soil and vegetative cover as well as continuous outcrops. Lava A1 erupted immediately following the ET1 eruption in 1968 and continues to the present day. Lava A2 erupted between Unit 10 and ET1, A3 between ET6 and ET7 and A4 between ET9B and ET9 (Ghigliotti et al., 1992). The designation LA, for lower Arenal, is given to lava samples whose stratigraphic position is not well defined but are likely older than A4. Thus, LA is not a distinct unit and will not be found in any stratigraphic plots. In addition to the lava flows, there are also minor explosions of lava bombs (Alvarado and Soto, 1997; Soto et al., 1998). These primarily occur between ET12 and ET13, ET13 and ET14, ET15 and ET16, and ET16 and SFB. The stratigraphy and ages of the lavas are listed in Table 1.

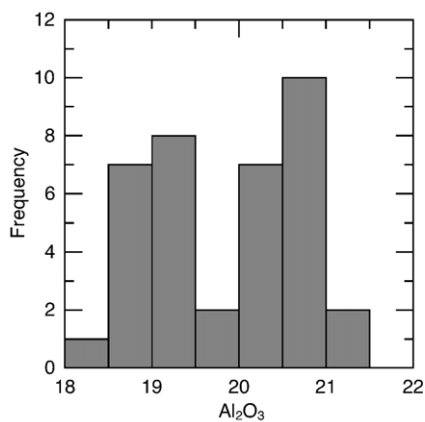


Fig. 2. Histogram of Al<sub>2</sub>O<sub>3</sub> for all lava flows and bombs analysed along with tephra unit ET1 and Unit 10. These two tephtra units are grouped with the lavas because their geochemistry resembles the lavas rather than the major tephtra units. ET1 is the tephtra that erupted first, clearing the way for the 1968 lava. It was likely the solidified cap over the magma that erupted as the 1968 lava.

Nearly all the lava flows are basaltic andesites with 54 to 56 wt.% SiO<sub>2</sub> (Borgia et al., 1988). They are classified into two groups based on their aluminum content. The high aluminum group (HAG) contains approximately 20.5 wt.% Al<sub>2</sub>O<sub>3</sub> whereas the low aluminum group (LAG) contains 18.5 wt.% Al<sub>2</sub>O<sub>3</sub> (Borgia et al., 1988). The lavas flows alternate between LAG and HAG. Lavas A1, A3, and LA are LAG; lavas A2 and A4 are HAG. Fig. 2 shows this bimodal distribution which also occurs in the lava bombs found between the older tephtra units. A third lava group, with an intermediate aluminum composition (IAG), has a chemical composition between HAG and LAG, but a lower SiO<sub>2</sub> content, 54 wt.% (Borgia et al., 1988). This small group represents an early stage that precedes the HAG and/or LAG lavas (Borgia et al., 1988).

## 2. Tephtra collection and correlation

Our sample set includes tephtra sections from 8 localities (Fig. 1). In all cases our samples were from original field work that sought to clarify the stratigraphy or from reoccupation of sections discovered to be particularly comprehensive during the stratigraphic field work. Wherever possible, the tephtra samples consisted of several large individual lapilli, which were cleaned and visually sorted in the lab. Most samples selected for geochemistry consisted of five or fewer lapilli.

Tephtra sets CT (Cruce tephtra) and RET (Represa tephtra) were collected in 1982, prior to the current stratigraphic synthesis (see Soto and Alvarado, 2006-this volume). Consequently, some of the tephtra layers in those sections were incorrectly identified. Using MgO and SiO<sub>2</sub> concentrations, the samples were reassigned to their proper tephtra units. The CT7 and RET7 tephtras were reassigned to tephtra unit ET6, CT8 and RET8 tephtras to ET7, CT9 and RET9 tephtras to ET8, RET10 to ET9N, RET11a to ET9A and RET11b to ET9B.

Two tephtra layers, Unit 10 and ET1, are distinct from the rest because they are much less voluminous than the other tephtra units. The 1968 tephtra, ET1, has already been substantially removed. Unit 10, the next most recent tephtra eruption, is also a thin layer compared to the other tephtra units. These two minor tephtras are chemically more similar to lavas than to the major explosive tephtra units. In fact, the major element chemistry of each of these thin units is similar to the lavas they preceded.

### 2.1. Petrography

The basic mineralogy at Arenal consists of plagioclase, clinopyroxene, orthopyroxene, hornblende, olivine, and

magnetite. Lavas and tephtras consistently have a porphyritic to glomeroporphyritic texture. Some tephtras have banded texture suggesting magma mingling. Phenocrysts of calcic plagioclase ( $An_{94-45}$ ) are up to 2.5 cm long, some are reversely zoned, but usually the phenocrysts have normal and oscillatory zoning and are rich in inclusions of glass, clinopyroxenes and fluids. Augite is common as euhedral to anhedral microphenocrysts and phenocrysts as large as 2 mm. Euhedral orthopyroxene up to 1.5 cm is present, some with normal to reverse zoning. Olivine phenocrysts ( $Fo_{69-83}$ ) are rare (0–0.1%) and are rimmed by orthopyroxene. Hornblende, as large as 10 mm, are magnesio-hastingsite and pargasite and have ophacitized rims. Titanomagnetite microphenocrysts are present but rare. The intergranular, interstitial, hyalopilitic to pilotaxitic groundmass has microlites of intermediate plagioclase, hypersthene, augite, pigeonite, Fe–Ti oxides, rare amphibole, interstitial cristobalite, and glass of andesitic to rhyolitic composition.

Although the lavas and tephtras are mineralogically similar, they vary in their degree of crystallinity and vesicularity. The lavas are generally 50% to 60% crystalline, although less so at flow exteriors. Mafic tephtras are 40% to 50% crystalline, whereas silicic tephtras have only 0% to 20% crystals. Silicic tephtras do not have large vesicles, whereas the mafic tephtras have larger as well as a higher volume of vesicles, 15% to 35% (Bolge, 2000).

Bolge et al. (2004) found that a few of the tephtras from unit ET3 had suffered severe weathering effects. Weathering is also a problem with the older tephtras. The extremely weathered tephtras are easily identified in thin section. The plagioclase in these samples retained their crystal shape but were altered to clay minerals. Several samples were identified as being altered. These samples will be discussed in the weathering section.

Percentages of mineral phases for each tephtra and lava unit were calculated (Table 2). These percentages were based on point counts of 1000 points on a representative sample from each interval. Pyroxenes, olivines, hornblende, and opaques were collectively counted as mafic minerals, since their chemical makeup consists of many of the same cations. Groundmass consisted of glass, ash and microlites. For the samples that had suffered weathering induced mineral alterations, the original prealtered mineral was assumed in the point counts.

Modal analyses reveal temporal variation in phenocrysts and groundmass percentages (Fig. 3). Over time, the mafic tephtras, and to a lesser extent the lavas, are progressively more enriched in phenocrysts (plagioclase

Table 2

Point counts of a representative sample for each unit

Sample	SiO <sub>2</sub> (wt.%)	Groundmass		Phenocrysts	
		%	%	% Fe–Mg	%
		Groundmass	Plagioclase	silicates	Opaques
A1	55	40.0	45.0	14.0	1.0
A2	55	49.1	43.7	6.4	0.8
UNIT10	55	64.7	29.3	3.7	2.3
ET2	60	92.0	4.9	2.6	0.5
ET3	53	57.7	27.3	13.3	1.8
ET4	58	94.2	3.8	1.4	0.6
ET5	59	89.7	9.2	0.7	0.4
ET6	52	67.1	24.5	7.7	0.7
A3	56	56.6	29.5	11.6	2.3
ET7	59	78.7	17.5	3.4	0.4
ET8M	52	68.8	25.0	5.9	0.3
ET8B	52	71.4	22.5	4.7	1.4
ET9N	63	83.7	10.1	4.9	4.3
ET9A	54	72.2	21.5	5.5	0.1
ET9B	53	78.6	15.5	5.1	0.8
A4	55	63.2	36.6	0.1	0.1
ET9	54	86.4	10.2	2.6	0.8
ET10	54	69.2	17.3	12.3	1.2
LA	54	50.5	34.1	13.9	1.5
ET11	54	87.4	9.8	2.1	0.7
ET11	60	91.3	6.3	1.7	0.7
ET12	53	81.8	16.7	1.1	0.3
bomb12.5	55	71.9	21.0	6.2	0.9
ET13	54	82.8	13.0	4.0	0.2
bomb13.5	55	61.8	26.7	10.2	1.3
ET14	54	89.4	8.4	0.9	1.3
ET15	51	84.3	12.3	1.9	1.5
bomb15.5	54	67.3	21.9	9.2	1.6
bomb16.5	53	65.9	20.2	12.6	1.3
SFB	62	76.0	19.5	2.4	2.1
bombSFB	54	56.2	33.2	9.6	1.0

and mafic minerals) and depleted in groundmass. The temporal changes in modal mineralogy of the silicic tephtras are roughly a mirror image of the changes in the mafic tephtras. As the mafic tephtras become more crystalline, the silicic tephtras become less crystalline. Our interpretation of this change is based on the detailed study by Bolge et al. (2004) of ET3 and ET4, a thick mafic tephtra sequence that erupted after a thick silicic tephtra sequence. They concluded that an incompatible element enriched siliceous melt rose from the mafic magma (ET3) into the overlying silicic magma (ET4). We assume that this process is common at Arenal and that it has become more efficient over time, making the mafic tephtras more phenocryst-rich and the silicic tephtras more glass-rich. Modal data also clarify the difference between the HAG and LAG lavas especially in the percentages of mafic minerals. The LAG lavas have a higher percentage of mafic minerals than the HAG lavas.

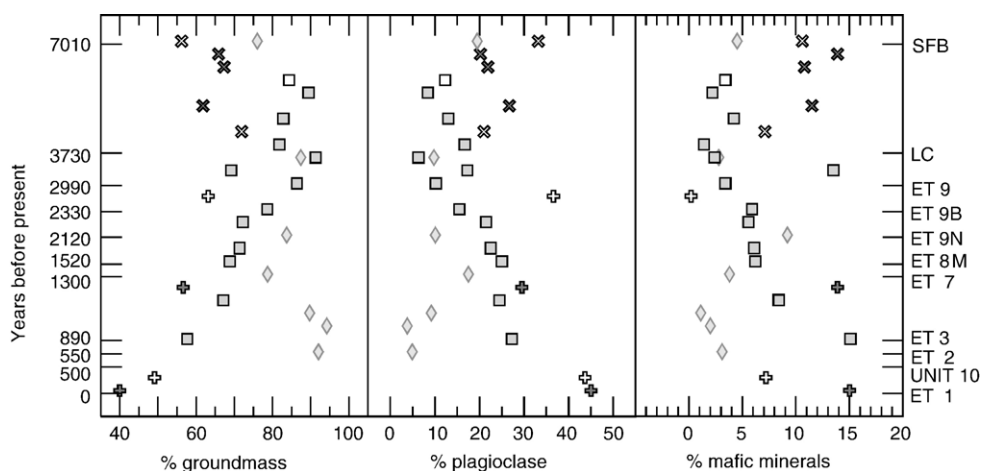


Fig. 3. Point counts show a decrease in groundmass and an increase in crystallinity in both the mafic tephtras and lavas over time. The silicic tephtras are a mirror image of the mafic tephtras. Filled squares are the mafic tephtras. Open squares are mafic tephtras affected by weathering. Filled diamonds are silicic tephtras. Filled crosses are HAG lavas, open crosses are LAG lavas, filled 'x's are HAG bombs, open 'x's are LAG bombs, filled curved crosses are ET1, open curved crosses are Unit 10.

Several types of enclaves (cumulates and xenoliths) occur in the lavas and pyroclastic deposits: (1) amphibole–olivine gabbros, (2) amphibole-free gabbroic cumulates (olivine gabbro, troctolite, and rare olivine clinopyroxenite), (3) olivine- and amphibole-free gabbronorites, anorthosites, and spinel granulites, known also as spinel pyriclasites (Beard and Borgia, 1989; Sacks and Alvarado, 1996; Cigolini, 1998). Megacrysts of anorthite ( $An_{96-90}$ ) rimmed by calcic plagioclase ( $An_{88-60}$ ), olivine ( $Fo_{81-71}$ ) and amphibolite occur in all rock types. Geobarometry suggests low to upper crustal depths for the crystallization of all enclaves (Cigolini and Kudo, 1987; Beard and Borgia, 1989). We also found anorthositic xenoliths or cumulates (77% plagioclase, 17% pyroxene and 6% opaques) in two samples from unit ET12. These completely crystalline lapilli were subordinate to the normal mafic lapilli found for this unit. In the field, they look identical to the normal lapilli because they are coated by an ashy rind. The crystalline lapilli were discovered only in thin section. Since thin sections were made for only a few lapilli from each interval, other crystalline lapilli may have been missed.

## 2.2. Geochemistry

All tephra and lava samples were analyzed for major and trace element compositions (see online database). In addition to the samples listed online, eight samples from unit ET1 taken from Alvarado et al. (2006-this volume) were also interpreted. This data set is an accumulation of several years worth of sample collection, consequently

major element data were analyzed by different instrumentation, DCP-AES (direct current plasma atomic emissions spectrometer) or XRF (X-ray fluorescence). All the major element data for a given sample were analyzed entirely by one of these two instruments. DCP-AES analyses were performed in the Department of Geological Sciences at Rutgers University. XRF analyses were made by the Department of Geological Sciences at Michigan State University. DCP-AES analyses report FeO total, while XRF analyses report  $Fe_2O_3$  total. The reader is referred to Feigenson and Carr (1985) for methods used for the DCP-AES analyses. For XRF methods, the reader is referred to the XRF website at Michigan State University ([http://geology.msu.edu/xrf\\_lab.html](http://geology.msu.edu/xrf_lab.html)).

All trace element analyses were performed on a Finnigan MAT High Resolution Inductively Coupled Plasma Mass Spectrometer (HR-ICP-MS) at the Institute of Marine and Coastal Sciences located at Rutgers University. Samples prepared for trace element analyses were digested using a HF/8 N  $HNO_3$  mixture, followed by additional fluxes of 8 N  $HNO_3$ . For more detailed methods, the reader is referred to Bolge (2005). Along with each batch of 12–15 samples a digestion blank and a USGS rock standard, either BHVO-1, AGV-1, or RGM-1, were also digested to check any possible contamination as well as the precision and accuracy of the digestion process. Although AGV-1 best represents the composition of the samples analyzed, BHVO-1 and RGM-1 certainly bracket the entire chemical range of the samples. Standard addition curves consisted of four points and had  $R^2$  values of 0.999 or

better. Average slopes of the standard curves were used to calculate concentrations. An average digestion blank for each run was also calculated and subtracted from all the samples. The digestion blanks were generally low and constant from blank to blank. Replicate digests of samples and USGS standards measured the precision of the entire digestion/preparation process. The USGS standards were also used to measure the accuracy of the analyses. Since there is no clear consensus on which preferred values are used for many of the trace elements, different labs tend to use their own accepted values for these rock standards. By using synthetic multi-element standards rather than USGS rock standards to standardize, USGS rock concentrations we measured can be used by others to normalize this data set to whatever their individual preferred values are. The measured values for these USGS rock standards along with their precision and the average blanks are also listed in the online database. For all geochemical plots the error bars on each element or elemental ratio is smaller than the symbol size.

Sr, Nd and Pb isotopes were also analyzed for a representative sample from each tephra and lava unit. These analyses were performed on a Micromass VG mass sector TIMS (Thermal Ionization Mass Spectrometer) or a GV Isoprobe T, both in the Department of Geological Sciences at Rutgers University. The reader is referred to Bolge (2005) for a detailed method. These isotopic data are listed in Table 3.

### 2.3. Identification and exclusion of weathered and questionable samples

Thin sections have shown the extensive weathering some of the tephtras have endured. Weathering has likely disturbed most if not all of the tephtras to some extent, affecting some elements much more than others. Since the tephtras are generally only a few centimeters in diameter and extremely porous, weathering is inevitable, especially given the hot wet Costa Rican climate. Before making any geochemical interpretations, samples that have been obviously

Table 3  
Isotopic composition of a representative sample for each unit

Sample	Description	$^{87}\text{Sr}/^{86}\text{Sr}$	$^{143}\text{Nd}/^{144}\text{Nd}$	$^{206}\text{Pb}/^{204}\text{Pb}$	$^{207}\text{Pb}/^{204}\text{Pb}$	$^{208}\text{Pb}/^{204}\text{Pb}$
A1	Lava flow	0.703890	0.513020	18.953+2	15.547+4	38.629+8
ET1	Tephra					
A2	Lava flow	0.703836+5	0.512993+16	18.983+2	15.548+3	38.688+8
UNIT10	Tephra					
ET2	Tephra	0.703821+7		19.027+3	15.571+2	38.821+6
ET3	Tephra	0.703808+6	0.512997+10	18.892+9	15.591+12	38.540+35
ET4	Tephra	0.703798+5	0.513004+16	18.975+2	15.665+2	38.965+6
ET5	Tephra	0.703805+7	0.513034+6	18.939+1	15.551+1	38.657+2
ET6	Tephra	0.703814+4	0.513014+2			
A3	Lava flow	0.703810+17	0.513013+21	18.874+4	15.571+8	38.599+15
ET7	Tephra	0.703811+21		19.043+2	15.572+2	38.823+4
ET8M	Tephra		0.513003+3	18.942+3	15.546+2	38.660+5
ET8B	Tephra	0.703882+9	0.513027+12			
ET9N	Tephra	0.703847+6	0.513001+5	19.051+1	15.561+1	38.833+3
ET9A	Tephra			18.899+1	15.553+1	38.623+2
ET9B	Tephra			18.999+11	15.598+10	38.822+24
A4	Lava flow	0.703817+4	0.513003+8	18.956+8	15.601+6	38.799+16
ET9	Tephra	0.703807+4	0.512975+14	19.225+51	15.725+47	39.327+116
ET10	Tephra	0.703831+4		18.971+2	15.575+1	38.760+3
LA	Lava flow	0.703821+18	0.512999+23	18.981+3	15.555+3	38.734+6
ET11	Tephra		0.513009+3	19.194+24	15.754+19	39.326+48
ET12	Tephra	0.703871+4		19.066+1	15.577+0	38.865+2
bomb12.5	Lava bomb		0.513015+3	19.057+1	15.567+1	38.840+3
ET13	Tephra		0.512979+5	19.055+3	15.552+3	38.829+7
bomb13.5	Lava bomb			19.181+20	15.679+17	39.241+44
ET14	Tephra	0.703817+4	0.513003+9	18.988+1	15.558+1	38.73+2
ET15	Tephra	0.703832+5	0.512997+3	19.061+1	15.549+1	38.815+3
bomb15.5	Lava bomb	0.703807+4		18.742+5	15.587+4	38.606+10
bomb16.5	Lava bomb	0.703795+16	0.512995+9	18.870+8	15.630+6	38.826+16
SFB	Tephra	0.703819+11				
bombSFB	Lava bomb	0.703806+4		18.957+2	15.565+2	38.717+4

modified by post magmatic processes need to be identified.

We identify compromised samples by plotting Ce vs. Ce\* (Fig. 4). In aqueous conditions, Ce is often removed preferentially to the other REE because it has an additional oxidation state, +4, in which Ce is more fluid mobile. Ce\* is the calculated concentration that Ce should have if the REE pattern follows a smooth transition from La to Pr, the two elements on either side of Ce. Using this discriminant we identified the following compromised samples: cas11, cas14, et-79-14, and cas15. Sample cas15, which shows a significant negative Ce anomaly, is likely too weathered to be used in any interpretations. Of the samples identified as weathered, three had thin sections made (cas11, cas14, cas15). All three of these samples showed significant clay alterations in their plagioclase.

Bolge et al. (2004) used a plot of Cs/Rb vs. K/Ba to identify several outlying samples which showed weathering effects in thin section in the extensively sampled ET4 and ET3 units at the Cruce section. Assuming a cogenetic source, these ratios should be very similar for all samples. Scatter on this plot results from the disproportionate removal and addition of these fluid mobile elements. Cs is the most mobile, then Rb, then K (this follows cation size, largest to smallest), and finally Ba (alkali earth elements are harder to mobilize under aqueous conditions than alkali elements). Bolge et al. (2004) showed that the thin sections with the most weathering were the samples with the largest variations in Cs/Rb and K/Ba. Using this discriminant, we added to the samples determined as weathered by Bolge et al.

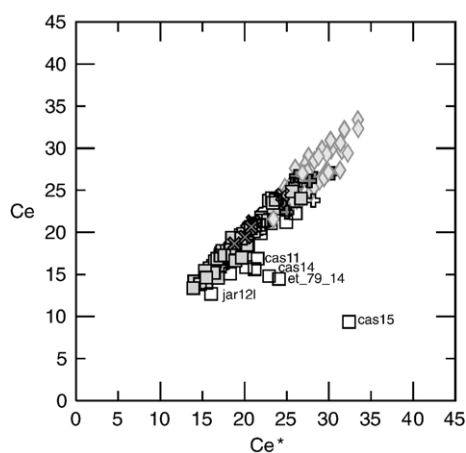


Fig. 4. Ce\* is the extrapolated value for Ce calculated from normalized La and Pr values. Samples off the 1:1 Ce/Ce\* line display the Ce anomalies caused by intensive weathering. The most severely weathered samples in this sample set have had Ce removed. Symbols are the same as in Fig. 3.

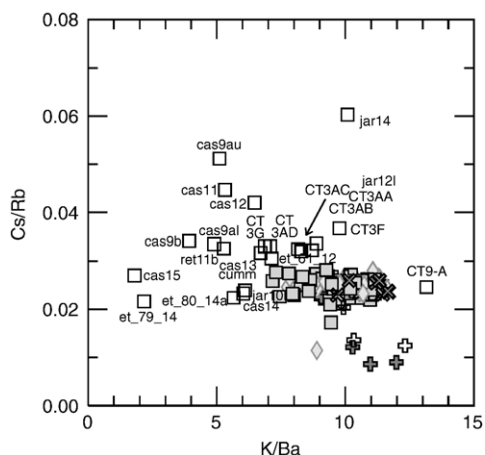


Fig. 5. The dispersion of the ratios Cs/Rb and K/Ba display which tephras have been weathered. These are ratios of fluid mobile elements. If samples are cogenetic, they should plot together. Scatter from the bulk of the sample distribution is the result of these elements being preferentially removed or added by weathering processes. Those samples showing the greatest scatter are the most severely weathered samples identified in Fig. 4. Symbols are the same as in Fig. 3.

(2004), 14 samples from our new sample set: ct9-A, cas9au, cas9al, cas9b, ret11b, jar10l, cas11, cas12, et-61-12, cas13cumm, jar14, et-79-14, et-80-14a, cas14 and cas15 (Fig. 5). As found in the Bolge et al. (2004) study, the samples with the most extreme weathering effects show the largest variations from the cluster of unweathered samples.

It is important to note that the discrimination plots only identify extensively weathered tephtras. All the

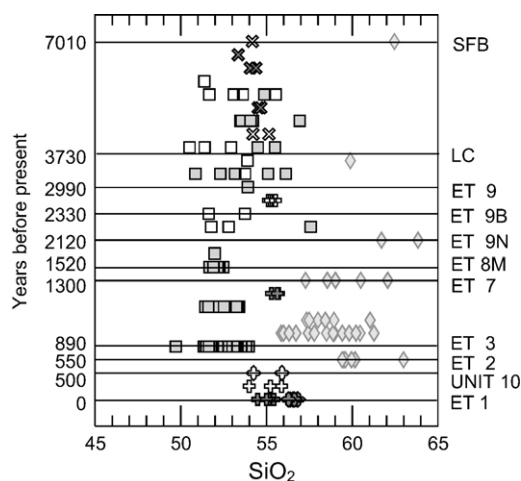


Fig. 6. Tephtras and lavas plotted as bulk SiO<sub>2</sub> composition versus relative stratigraphy showing the amount of weathered samples for each unit. The plotted SiO<sub>2</sub> has been normalized to 100 wt.%. Calibrated ages for each tephtra unit are taken from Soto and Alvarado (2006-this volume).

tephras have likely undergone some degree of alteration. In an attempt to see through the alterations, and make robust interpretations of the magmatic history we stress the elements that are immobile in fluids (HFSE and HREE). Wherever possible fluid mobile elements such as Li, Na, K, Rb, Cs, Ba, La, Ce, Th, U, Tl, and Pb are not used. Because we rely on fluid immobile elements, some samples identified as weathered are still used. A primary reason for retaining some weathered samples is that many of the older tephra units are entirely represented by samples with recognizable weathering, e.g. ET9A, ET9B and ET11. Fig. 6 shows the number of samples in each unit as well as how many of the samples show alteration.

### 3. Silica content

Previous studies of Arenal's stratigraphy discovered an alternation between silicic ( $57 < \text{wt.}\% \text{SiO}_2 < 59$ ) and mafic ( $51 < \text{wt.}\% \text{SiO}_2 < 53$ ) tephras during the last 3000 years, from unit ET9 to ET2 (Melson, 1982, 1984, 1994). However, the tephras erupted prior to ET9 are unimodal ( $53 < \text{wt.}\% \text{SiO}_2 < 55$ ), lacking the alternation of mafic and silicic units so prominent in the uppermost stratigraphy. The transition from unimodal to bimodal tephra stratigraphy occurred below unit ET9 at about 3000 years B.P. (Fig. 6).

We must note, however, that there is one silicic sample in these early tephra units. ET11 is represented by two samples, one a mafic tephra and the other a silicic tephra. Since both tephra types were found within this layer, the silicic tephra is likely the result of crystal fractionation within this magma. The oldest known eruption of Arenal, SFB, is also silicic with mafic lava bombs within it. This initial eruption at Arenal is significantly larger than the older (pre-ET9) tephras. It should not be grouped together with the other ET layers. Its silicic composition likely resulted from substantial differentiation prior to the initial eruption of Arenal.

Our current work divides the Arenal eruptives into four groups (Fig. 7a–c), the early less voluminous unimodal tephras with a prominent peak at 53–55 wt.%  $\text{SiO}_2$ ; recent voluminous bimodal tephras, with mafic (51–55 wt.%  $\text{SiO}_2$ ) and silicic (56–64 wt.%  $\text{SiO}_2$ ) subgroups; and finally lavas and proximal bombs (54–57 wt.%  $\text{SiO}_2$ ). The bombs have similar chemistry to the lavas as well as the two most recent tephras, ET1 and Unit 10, which were the result of extremely hazardous but low volume directed blasts.

We estimate the volume of lavas erupted from Arenal's cones to be about  $15 \text{ km}^3$ . The tephra volumes are less, about  $4.5\text{--}5 \text{ km}^3$  in total. Individual mafic

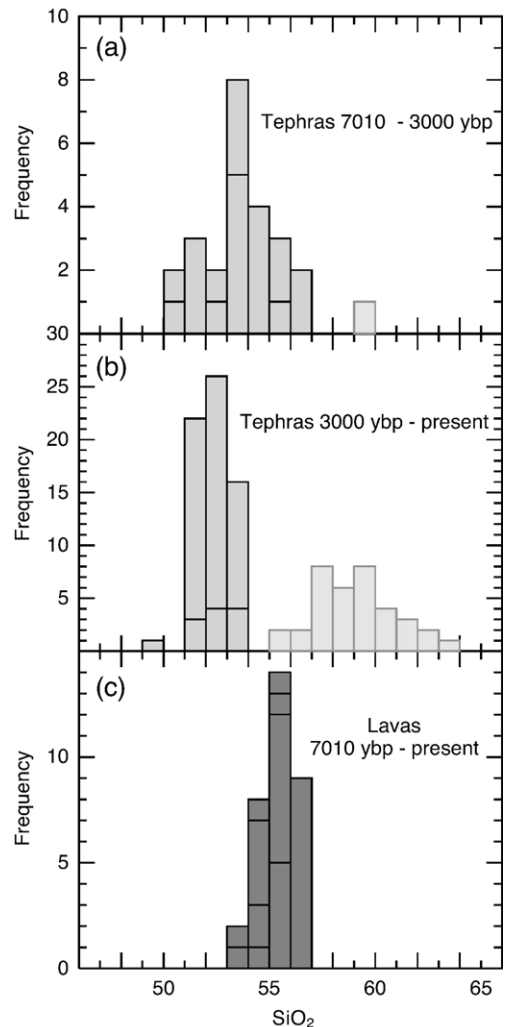


Fig. 7. (a) Tephras erupted between 7010 and 3000 years B.P. show a relatively unimodal  $\text{SiO}_2$  composition with one sample from unit ET11 with an elevated  $\text{SiO}_2$ . (b) Tephras erupted between 3000 years B.P. and the present show a bimodal distribution of  $\text{SiO}_2$ . (c) The lavas erupted during Arenal's entire history show a unimodal  $\text{SiO}_2$  distribution that is similar to that of the older tephras (a) and lie in the gap between the bimodal distribution of the younger tephras. The plotted  $\text{SiO}_2$  has been normalized to 100 wt.%.

tephras are on average  $0.2 \text{ km}^3$  and silicic tephras are on average about  $0.4 \text{ km}^3$  (Soto and Alvarado, 2006-this volume), significantly smaller than the volume of the presently erupting lava unit. Allowing for the actual volumes of the lava and tephra units, the distribution of  $\text{SiO}_2$  contents at Arenal is unimodal and centered on the lavas at about 54 to 57 wt.%  $\text{SiO}_2$  (Fig. 7c).

Both the modal and geochemical data argue that Arenal is experiencing more crystal–liquid sorting in a magma chamber over time. Over time, the mafic tephras, and to a lesser extent the lavas, are becoming

more crystalline, while the silicic tephtras are becoming less crystalline. Although the efficiency of crystal–liquid fractionation at Arenal has an abrupt increase at 3000 years B.P., this is superimposed on a gradual increase in fractionation efficiency throughout Arenal’s 7000-year history. This gradual change is demonstrated well in the mafic tephtras since they show the most complete history. Prior to 3000 years B.P., the efficiency of crystal–liquid fractionation was considerably less, resulting in a unimodal tephtra composition with a mean  $\text{SiO}_2$  composition identical to that of the contemporaneous lavas and bombs. At approximately 3000 years B.P. the volcano reaches a threshold where silicic tephtras begin to be produced consistently in conjunction with the mafic tephtras. At this point a clear separation in  $\text{SiO}_2$  content between the tephtras and lavas develops. If a basaltic andesite is the replenishing magma input into the Arenal system, based on the lava compositions, then the younger basaltic tephtras are consistent with a residue, enriched in mafic minerals after a silicic melt is extracted (Bolge et al., 2004). With increased crystal–liquid separation, the silicic tephtras reach  $\text{SiO}_2$  contents of almost 65 wt. %.

### 3.1. Temporal variations in elemental concentrations

Temporal geochemical variations in the mafic tephtra units should be the result of an increase in the amount of phenocrysts and concomitant decrease in the amount of groundmass. Because there is some variation within individual tephtra layers (Bolge et al., 2004) we use mean values for each unit to show the temporal changes in elemental or oxide composition. Plagioclase is the

most abundant phenocryst mineral in the tephtras with clinopyroxene, orthopyroxene, olivine, hornblende, and opaque minerals making up the remaining mineralogy. The elements compatible in one or more of the phenocrysts (MgO, CaO, Sr, Sc, V, Cr, Co, Ni, Cu, and Mo) generally increase over time as the modal percentage of these minerals increases (e.g., Fig. 8).

The inventory of incompatible elements is held primarily in the groundmass (consisting of glass, ash, and microlites). The decrease in groundmass with time should lead to lower incompatible element concentrations in the mafic tephtras. Concentrations of incompatible elements (Y, Zn, Zr, Hf, Nb, Ta and the REE elements from Pr through Lu) decrease with time as expected from the decreasing groundmass content of the mafic tephtras (e.g., Fig. 9).

Looking solely at the mafic tephtras, the redistribution of phenocrysts is causing the temporal geochemical trends. However, the silicic tephtras, which are a mirror image of the mafic tephtras in modal mineralogy, show the same temporal geochemical trends. The concentrations of the compatible elements increase over time, while the incompatible elements decrease. This cannot be explained by phenocryst redistribution since the silicic tephtras have fewer phenocrysts over time.

The answer to this paradox lies within the lavas. Over the past 7000 years, the bombs and lavas of Arenal have become more enriched in incompatible elements;  $\text{K}_2\text{O}$ , Rb, La, Ce, Ba and Sr (e.g., Fig. 10). These elements have a strong positive correlation with  $\text{SiO}_2$ , which also increases with time. The increase in  $\text{SiO}_2$  is only from about 54 wt. % to about 56 wt. %. Over time at Arenal the lavas are becoming more enriched in incompatible

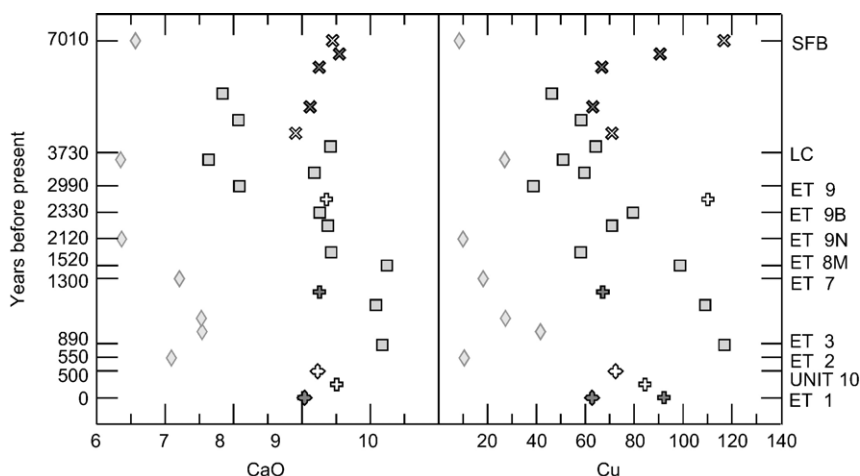


Fig. 8. An average value for each tephtra unit is used to limit the amount of dispersion seen within the individual unit from fractionation. The concentration of compatible elements increases over time for both the mafic and silicic tephtras. Symbols are the same as in Fig. 3.

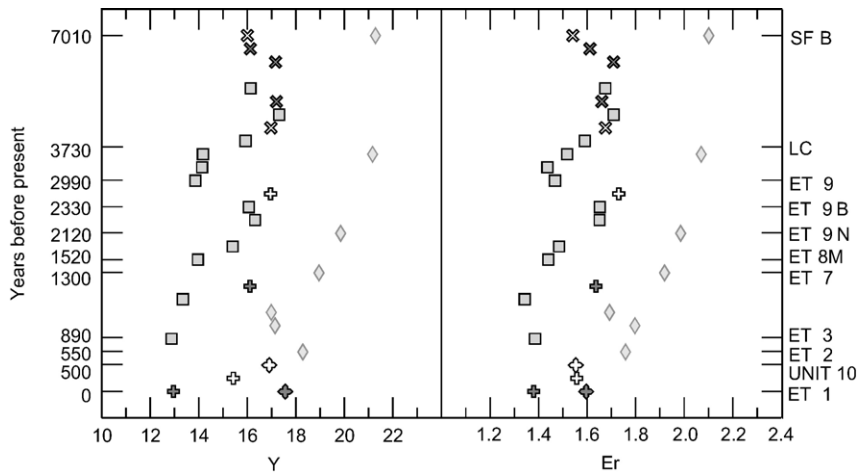


Fig. 9. An average value for each tephra unit is used to limit the amount of dispersion seen within the individual unit from fractionation. The concentration of incompatible elements decreases over time for both the mafic and silicic tephras. Symbols are the same as in Fig. 3.

elements while the tephtras, both mafic and silicic, are becoming more enriched in compatible elements.

Although the lava flows and bombs (those from small volume eruptions) can be further subdivided into HAG and LAG groups, there appears to have been no change in the HAG–LAG dichotomy (Fig. 2) over time except that the separation has become clearer. The suggestion by Borgia et al. (1988) that the scarce IAG group is parental to the other Arenal volcanic is supported by the discovery of many bombs of similar composition in the subsequently discovered pre-ET9 stratigraphy. The alternation between HAG and LAG is the reason that we cannot see a decrease in compatible elements.

In addition to the increase in crystal–liquid redistribution seen very well in the percentage of phenocrysts

and groundmass for both the tephtras and lavas over time, there is also redistribution not only within the tephtras and lavas, but also between these two eruptive products. Over time more of the incompatible elements are being removed from the part of the magma that will erupt as tephtras to the magma that will erupt as lavas, or more compatible elements are being removed from the lavas to the tephtras. Since the volume of tephtras erupted is so much smaller than that of the lavas these geochemical temporal changes are much easier to see in the tephtras, as opposed to the change in the lavas which is very subtle.

### 3.2. Degree of melting

Plots of stratigraphic position versus Zr/Hf and to a lesser extent Nb/Ta (Fig. 11) indicate that the degree of melting at Arenal changes with time. These elements are used for two reasons; first, they are resistant to weathering, and second, because only very small degrees of melting can fractionate Zr from Hf and Nb from Ta. In these ratios, the numerators, Zr and Nb, are slightly more incompatible than the denominators, Hf and Ta and, consequently, lower Zr/Hf and Nb/Ta indicate higher degrees of melting. The degree of melting steadily increased until approximately 3000 years B.P. It then decreased until about 500 years B.P. and now is increasing again. Because these changes are within the partial melting region in the mantle, both tephtras and lavas are affected.

The stratigraphic variation in Zr/Hf is clear but the variation in Nb/Ta is clear only for the younger part of the section. The cause for the high dispersion in Nb/Ta

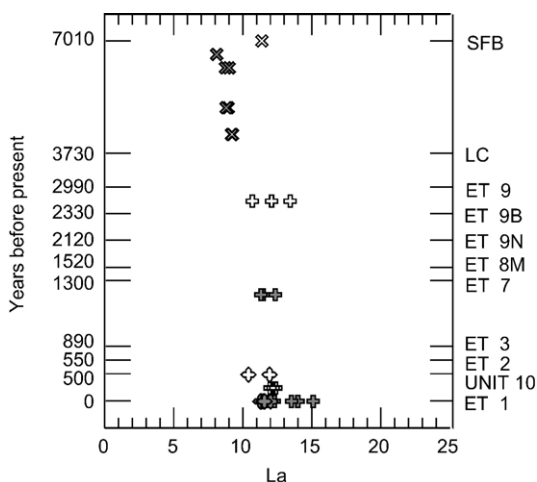


Fig. 10. The concentration of incompatible elements, such as La, increases over time in the lavas. Symbols are the same as in Fig. 3.

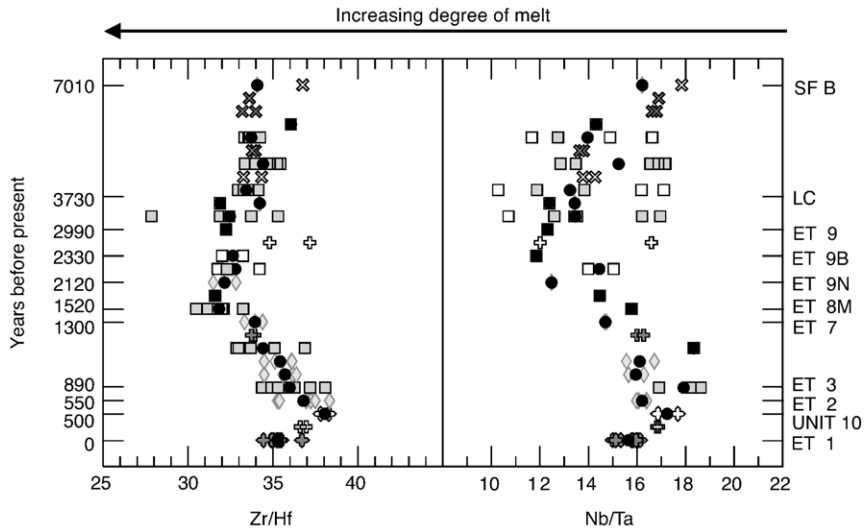


Fig. 11. Zr/Hf and to a lesser extent Nb/Ta show an increase in the degree of melting over time up to approximately 3000 years B.P., followed by a steady decrease from then to the present. The Nb/Ta data in the older tephras show variation due to the large variation in the TiO<sub>2</sub> relative to the younger tephras. Average values for the tephras are presented as filled black circles. All other symbols are the same as in Fig. 3.

for the older tephras appears to be a combination of fractionation and weathering that affects only the tephras. Within these samples, there is a weak positive correlation of Nb/Nb\* with Ce/Ce\* ( $r=0.59$ ), suggesting that weathering has started to lower the Nb contents of the mafic tephras. Nb\* is a value calculated much like Ce\*. Nb in arc systems shows a depletion relative to elements of similar incompatibility. This can be seen on spider diagrams. Nb\* is the calculated value for Nb

if there was no depletion. This value is based on the elements on either side of Nb on a spider diagram, U and K. Similarly, after removing the more weathered mafic tephras, there is a weak positive correlation of Nb/Ta with TiO<sub>2</sub> ( $r=0.53$ ), suggesting fractionation of Nb/Ta by a titanium bearing mineral. However, ignoring the older tephras and instead focusing on the bombs from this time period, Nb/Ta follows the same pattern as Zr/Hf.

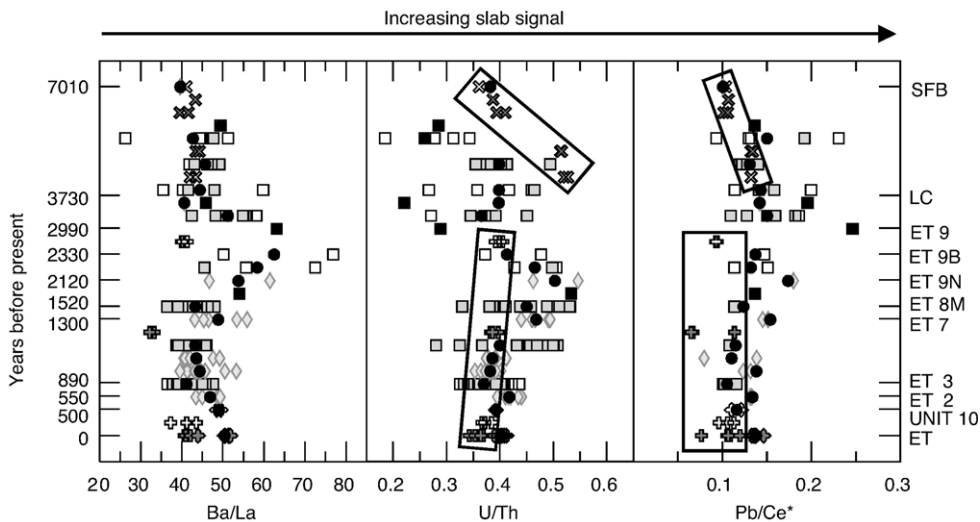


Fig. 12. Ba/La, U/Th and Pb/Ce are traditionally used as proxies for slab signal. The tephras show an increase in slab signal at approximately 3000 years B.P. However, these ratios contain fluid mobile elements and therefore the tephra compositions are likely skewed. Plots of U/Th and Pb/Ce\*, however, show two distinct trends in the lavas, one in the older bombs and one in the younger lava flows. The offset between these two trends occurs at approximately 3000 years B.P. Symbols are the same as in Fig. 11.

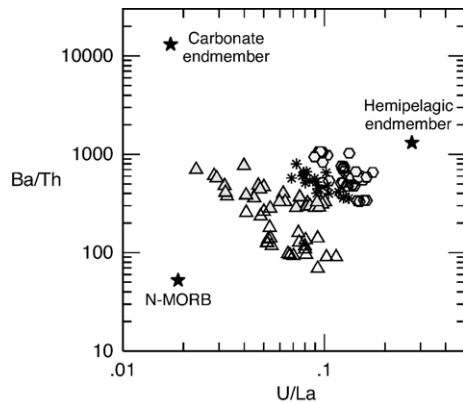


Fig. 13. Central American data taken from Bolge (2005) showing the two sedimentary endmembers defined by the ratios Ba/Th and U/La and their effect on Central American lavas. Asterisks are El Salvador. Filled hexagons are Northern Nicaragua. Empty hexagons are Southern Nicaragua. Filled triangles are Northern Costa Rica. Empty triangles are Central Costa Rica.

### 3.3. Amount of subducting slab

In addition to the change in the degree of melting, there is also a change in the strength of subducted slab signal. The ratios, Ba/La, U/Th and Pb/Ce (Fig. 12) are proxies for the slab signal. These ratios are much higher in the slab components being subducted than they are in the mantle. For each ratio, the paired elements are roughly equal in their compatibilities in melts. The numerator in each ratio is more fluid mobile than the denominator. As more slab derived

fluids enter the mantle wedge, these ratios will increase. The amount of slab component reaches a maximum around 3000 years B.P.

The change in the amount of slab signal (e.g. Ba/La in Fig. 12) is roughly a mirror image of the change in the degree of melting (Zr/Hf in Fig. 11). A higher concentration of fluids from the slab into the overlying mantle wedge would produce higher degrees of melting. Therefore, the changes in source composition are primarily caused by variations in the amount of slab component.

Since fluid mobile elements have likely been compromised by weathering in the tephtras, the plots in Fig. 11 must be interpreted with caution. However, the lavas (highlighted by the rectangles) do not suffer as much alteration as the tephtras and they do shift to higher U/Th and Pb/Ce\* at approximately 3000 years ago.

Two distinct sedimentary components in the Cocos Plate subduct beneath Central America, a basal carbonate layer, overlain by a hemipelagic layer. The ratios Ba/Th and U/La (Fig. 13) have been used to separate these two components (Patino et al., 2000). The carbonate endmember has high Ba/Th, whereas the hemipelagic component has elevated U/La. Ba/Th, shows no obvious change throughout Arenal's history (Fig. 14), whereas U/La (Fig. 14) has a temporal variation similar to that of Ba/La (Fig. 12). Once again the use of fluid mobile elements makes it important to focus on the lavas, which for U/La, are in fact following the same temporal pattern as the tephtras. Therefore, the similar variation in Ba/La, U/Th and Pb/Ce\* with U/La over time, implies that

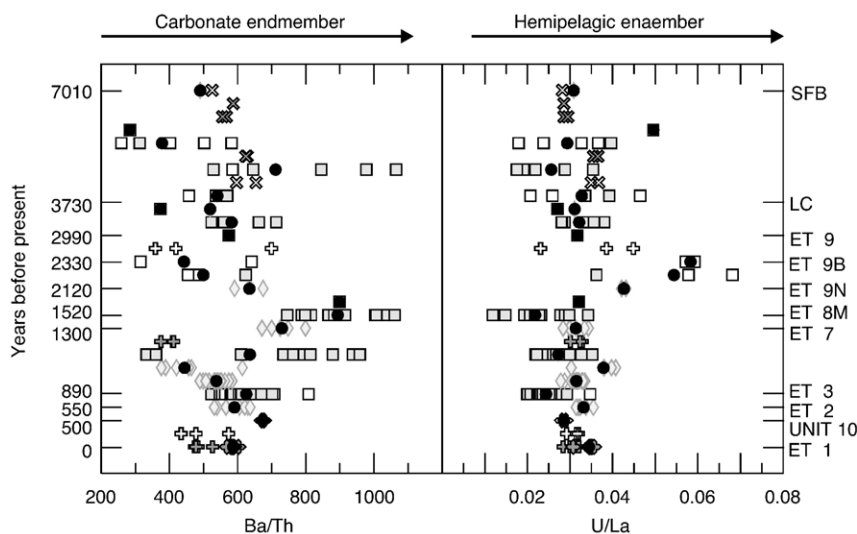


Fig. 14. The carbonate sedimentary endmember (Ba/Th) shows no discernable trends, while the hemipelagic sedimentary endmember (U/La) shows the same increase at approximately 3000 years B.P. as the bulk slab signal seen in Fig. 12. Symbols are the same as in Fig. 11.

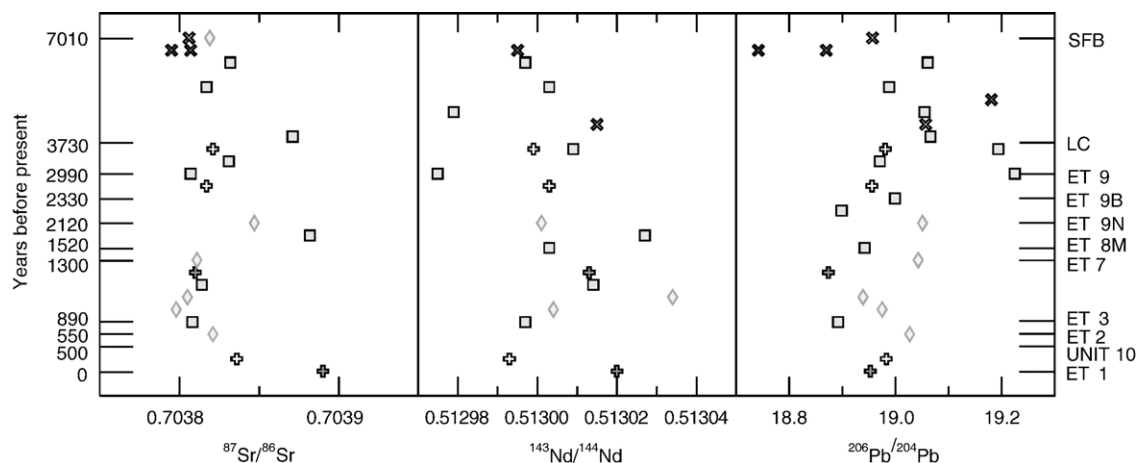


Fig. 15. Sr and Nd isotopes show a possible increase at approximately 3000 years B.P. supporting an increase in slab signal. Pb isotopes show no temporal variation. Symbols are the same as in Fig. 3.

variations in slab component are primarily the result of changes in the amount of hemipelagic sediment. Although the carbonate sedimentary layer is a major slab component, it is not causing the changes in the source region beneath Arenal.

### 3.4. Isotopic data

There is a slight elevation in the  $^{87}\text{Sr}/^{86}\text{Sr}$  and  $^{143}\text{Nd}/^{144}\text{Nd}$  composition around ET8B (Fig. 15). Both isotopic compositions are lower for younger and older samples. All the subducted components have elevated isotopic ratios, however, this elevated  $^{87}\text{Sr}/^{86}\text{Sr}$  is also seen in the most recent lava A1 where the slab flux is low. We also obtained Pb isotope ratios, which showed no overall temporal change, however tephra units ET9 and ET11 do have elevated  $^{206}\text{Pb}/^{204}\text{Pb}$ .

## 4. Conclusions

Arenal's magma is experiencing more crystal–liquid fractionation over time. Both the mafic tephtras and lavas are becoming more crystalline. This increase in fractionation efficiency reaches a threshold at approximately 3000 years B.P., where silicic tephtras begin to be produced consistently in conjunction with the mafic tephtras. Prior to this change, the mafic tephtras overlapped in  $\text{SiO}_2$  concentration with the lavas.

Both the mafic and silicic tephtras show increases in the concentration of compatible elements and decreases in incompatible elements over time. The lavas to a lesser extent show the opposite temporal trends. This demonstrates that not only is there an increase in the efficiency of the crystal–liquid separation and redistribution over

time within the tephtras and lavas, but also between these two eruptive products.

There have been changes in the source region beneath Arenal, most prominent a maximum in the degree of melting at approximately 3000 years B.P. A change in the amount of flux from the subducting slab most likely caused the change in the melting regime at Arenal. The amount of flux and consequently the degree of melting increase from 7000 years B.P. to a maximum at approximately 3000 years B.P. then both decrease to the present. The changes in the flux appear to have primarily been from the hemipelagic section of the Cocos Plate stratigraphy.

The temporal changes in the geochemistry and petrology of Arenal's eruptive products reflect crystal–liquid sorting, new magma input at crustal levels and deeper processes. The deeper processes include changes in the relative proportions of source components and changes in the degree of melting, which occur either in the mantle wedge or at the subducting slab.

## Acknowledgements

This work was partially supported by National Science Foundation Grants NSF EAR-0203388 and NSF EAR-9905167. We thank Francisco (Chico) Arias and Kathy Milidakis for their help in the field.

## Appendix A. Supplementary data

Supplementary data associated with this article can be found, in the online version, at [doi:10.1016/j.jvolgeores.2006.03.036](https://doi.org/10.1016/j.jvolgeores.2006.03.036).

## References

- Alvarado, G.E., Soto, G.J., 1997. Aspectos petrológicos de las Tefras del Arenal Volcánico. Bol. OSIVAM 7 (13–14), 58–72.
- Alvarado, G.E., Soto, G.J., Schmincke, H.U., Bolge, L.L., Sumita, M., 2006-this volume. The 1968 lateral blast eruption at Arenal Volcano, Costa Rica. *J. Volcanol. Geotherm. Res.* 157, 9–33. doi:10.1016/j.jvolgeores.2006.03.035.
- Beard, J.S., Borgia, A., 1989. Temporal variation of mineralogy and petrology in cognate gabbroic enclaves at Arenal volcano, Costa Rica. *Contrib. Mineral. Petrol.* 103, 110–122.
- Bolge, L.L., 2000. Geochemistry of tephros from Arenal Volcano, Costa Rica: Repeated cycles of explosive volcanism. MS thesis, Rutgers Univ. New Brunswick, NJ, USA.
- Bolge, L.L., 2005. Constraining the magmatic sources of Hawaiian and Central American volcanics. PhD thesis, Rutgers Univ. New Brunswick, NJ, USA.
- Bolge, L.L., Carr, M.J., Feigenson, M.D., Borgia, A., 2004. Geochemistry and magmatic evolution of explosive tephros ET3 and ET4 from Arenal Volcano, Costa Rica. *Rev. Geol. Am. Cent.* 30, 127–135.
- Borgia, A., Poore, C., Carr, M.J., Melson, W.G., Alvarado, G.E., 1988. Structural, stratigraphic, and petrologic aspects of the Arenal–Chato volcanic system, Costa Rica: evolution of a young stratovolcanic complex. *Bull. Volcanol.* 50, 86–105.
- Cigolini, C., 1998. Intracrustal origin of Arenal basaltic andesite in the light of solid–melt interactions and related compositional buffering. *J. Volcanol. Geotherm. Res.* 86, 277–310.
- Cigolini, C., Bogliotti, C., 1984. Phase relationship and “silicate liquid immiscibility” in Arenal Volcano lavas, Costa Rica: preliminary studies. *Atti Accad. Sci. Torino* 118, 226–236.
- Cigolini, C., Kudo, A.M., 1987. Xenoliths in recent basaltic andesite flows from Arenal Volcano, Costa Rica: inference on the composition of the lower crust. *Contrib. Mineral. Petrol.* 96, 381–390.
- Feigenson, M.D., Carr, M.J., 1985. Determination of major, trace and rare earth elements in rocks by DCP-AES. *Chem. Geol.* 51, 19–27.
- Ghigliotti, M., Frullani, A., Alvarado, G.E., Soto, G.J., 1991. Distribucion areal y características de los depositos de tefra mas recientes (1080–1968 dC) del Volcan Arenal. *Bol. Obs. Vulcanol. Arenal* 4 (8), 11–33.
- Ghigliotti, M., Frullani, A., Soto, G.J., Alvarado, G.E., 1992. Tefrostratigrafia, historia y ciclos eruptivos del volcan Arenal. *Bol. Obs. Vulcanol. Arenal* 5 (9–10), 52–96.
- Kussmaul, S., Paniagua, S., Gainza, J., 1982. Recopilación, clasificación e interpretación petroquímica de las rocas ígneas de Costa Rica. *Inf. Semest.-Inst. Geogr. Nac.* 28, 17–79 (Julio–Diciembre).
- Malavassi, E., 1979. Geology and petrology of Arenal Volcano, Costa Rica. MS thesis, Univ of Hawaii.
- Melson, W.G., 1982. Alternancia entre magmas acido y basicos en las erupciones explosivas mayores del Volcan Arenal, Costa Rica. *Bol. Vulcanol.* 13, 65–74.
- Melson, W.G., 1984. Prehistoric eruptions of Arenal Volcano, Costa Rica. *Vinculos* 10, 34–59.
- Melson, W.G., 1994. The eruption of 1968 and tephra stratigraphy of Arenal Volcano. *Archaeology, Volcanism, and Remote Sensing in the Arenal Region, Costa Rica*, pp. 24–47.
- Melson, W.G., Saenz, R., 1973. Volume, energy and cyclicity of eruptions of Arenal Volcano. *Bull. Volcanol.* 37, 416–437.
- Patino, L.C., Carr, M.J., Feigenson, M.D., 2000. Local and regional variations in Central American arc lavas controlled by variations in subducted sediment input. *Contrib. Mineral. Petrol.* 138, 265–283.
- Reagan, M., Gill, J., Malavassi, E., Garcia, M., 1987. Changes in magma composition at Arenal volcano, Costa Rica, 1968–1985: real-time monitoring of open-system differentiation. *Bull. Volcanol.* 49, 415–434.
- Sacks, P.M., Alvarado, G.E., 1996. Mafic metaigneous lower crust beneath Arenal Volcano (Costa Rica): evidence from xenoliths. *Bol. Obs. Vulcanol. Arenal* 6 (11–12), 71–78.
- Soto, G.J., Alvarado, G.E., 2006-this volume. Eruptive history of Arenal Volcano, 7 ka to present. *J. Volcanol. Geotherm. Res.* 157, 254–269. doi:10.1016/j.jvolgeores.2006.03.041.
- Soto, G.J., Alvarado, G.E., Ghigliotti, M., 1998. El registro eruptivo del Arenal en el lapso 3000–7000 años antes del presente y nuevas deducciones sobre la edad del volcan. *Bol. OSIVAM* 9 (17–18), 19–49.
- Streck, M.J., Dungan, M.A., Malavassi, E., Reagan, M.K., Bussy, F., 2002. The role of basalt replenishment in the generation of basaltic andesites of the ongoing activity at Arenal Volcano, Costa Rica: evidence from clinopyroxene and spinel. *Bull. Volcanol.* 64, 316–327.
- Tournon, J., 1984. Magmatismes du Mesozoique à l’actuel en Amérique Centrale: l’exemple de Costa Rica, des ophiolites aux andésites. *Mémoires Sciences Terre*. PhD thesis, Univ. Pierre et Marie Curie, Paris.